Thematic Review Series: Applications in Lipid Metabolism, Transport, Homeostasis

Deep-lipidotyping by mass spectrometry: recent technical advances and applications

Wenpeng Zhang[1], Ruijun Jian[2], Jing Zhao[2], Yikun Liu[1], and Yu Xia[2]*

[1]State Key Laboratory of Precision Measurement Technology and Instruments, Department of Precision Instruments, and [2]MOE Key Laboratory of Bioorganic Phosphorus Chemistry & Chemical Biological, Department of Chemistry, Tsinghua University, Beijing, P. R. China

Abstract In-depth structural characterization of lipids is an essential component of lipidomics. There has been a rapid expansion of mass spectrometry methods that are capable of resolving lipid isomers at various structural levels over the past decade. These developments finally make deep-lipidotyping possible, which provides new means to study lipid metabolism and discover new lipid biomarkers. In this review, we discuss recent advancements in tandem mass spectrometry (MS/MS) methods for identification of complex lipids beyond the species (known headgroup information) and molecular species (known chain composition) levels. These include identification at the levels of carbon-carbon double bond (C=C) location and *sn*-position, as well as characterization of acyl chain modifications. We also discuss the integration of isomer-resolving MS/MS methods with different lipid analysis workflows and their applications in lipidomics. The results showcase the distinct capabilities of deep-lipidotyping in untangling the metabolism of individual isomers and sensitive phenotyping by using relative fractional quantitation of the isomers.

Supplementary key words lipidomics • tandem mass spectrometry • lipid isomers • double bond location • *sn*-position • glycerolipids • glycerophospholipids • branched-chain fatty acids • liquid chromatography • phenotyping

The systems approach to lipids, which aims to reveal a complete network of the function and metabolism of lipids, and their interactions with other biomolecules in a biosystem, came into shape as "lipidomics" in the early 2000s (1). Ever since, lipidomics has gradually emerged from being a subdiscipline of metabolomics into a more independent research field due to many differences in experimental approaches employed for the two cohorts of molecules (2). In the past decade, lipidomics has been increasingly employed in both basic and translational research, while the lipidomic data are found instrumental in understanding metabolic changes of many diseases, including COVID-19 (3, 4).

The advancement of lipidomics is supported by a variety of analytical techniques, especially mass spectrometry (MS), which provides a solution to large-scale lipid profiling. The development of state-of-the-art MS instruments, tandem mass spectrometry (MS/MS) methods tailored for lipid analysis, and the hyphenation of MS with high-performance separation methods are the three pillars underpinning the fast growth of lipidomics. This is witnessed by over 2000 publications in the year of 2020 from searching the Web of Science with key words, "lipidomics" or "lipid analysis + mass spectrometry", an almost two-fold increase from that of 2016 (https://www.webofscience.com/, 2022/01/03). Echoing the heated research activity was the establishment of the International Lipidomics Society in 2019, with a clear goal to foster the development of new technologies, resources, data standardization (5), and so forth (https://lipidomicssociety.org/).

This review is mainly focused on lipid identification, a rudimentary step to all lipid profiling experiments. The challenge of lipid identification stems from structural complexity and diversity. LIPIDMAPS curates more than 40,000 lipid molecules, which are classified into eight categories. Among them, fatty acids (FAs) are the building blocks of complex lipids, such as glycerolipids (GLs), glycerophospholipids (GPLs), and sphingolipids (SLs) (6). Conventionally, lipid extracts are analyzed by gas chromatography-electron ionization-mass spectrometry (GC-EI-MS) after saponification, in which the fatty acyls in complex lipids are hydrolyzed and esterified (7). This approach provides comprehensive profiling of total FAs from a given lipidome; however, the information of the intact structures of complex lipids is lost. Owing to the invention of soft ionization methods, namely electrospray ionization (ESI) and matrix-assisted laser desorption ionization (MALDI), complex lipids can be detected and structurally probed as a whole when coupled with MS/MS

*For correspondence: Yu Xia, xiayu@mail.tsinghua.edu.cn.

 https://doi.org/10.1016/j.jlr.2022.100219

methods (8, 9). These two approaches can be classified as the "bottom-up" and the "top-down" lipid analysis, respectively, analogous to the terminology used in proteomics.

Complete identification of a complex lipid, using a GPL molecule as an example, requires an elucidation on the following six structural levels (**Fig. 1**): 1) identity of the head group, 2) acyl composition, 3) location(s) of carbon-carbon double bond(s) (C=Cs), 4) *sn*-position of the acyl/ether chains on the glycerol backbone, 5) identity and location of functional group substitution (e.g., methyl branching and hydroxylation), and 6) the stereochemistry of C=Cs and the chiral centers. By employing high-resolution MS and MS/MS, information of the first two levels can be obtained from routine lipidomic profiling workflows. However, any variation at deeper structural levels (levels 3–6 in Fig. 1) leads to a plethora of isomeric structures that cannot be differentiated by mass measurements alone. So far, the high-performance separation methods are still struggling in providing a universal solution for the separation of lipid isomers. Moreover, due to a lack of synthetic standards, even though isomers are separated, they cannot be assigned to a specific structure.

The development of novel MS/MS techniques has been a valuable resource for characterizing biomolecules at high sensitivity. Notable examples in proteomics include using electron-based ion activation methods, i.e., electron-capture dissociation (11) and electron-transfer dissociation, (12) to locate the site of phosphorylation and electron-induced dissociation to assign the linkage patterns in glycans (13). Similarly, active research efforts have been drawn from the mass spectrometry society on developing new MS/MS methods for top-down lipid analysis over the last decade, establishing deep-lipidotyping as an important tool for structural lipidomics (14). Figure 1 summarizes the published MS/MS methods for retrieving each level of lipid structural information and corresponding nomenclature suggested by Liebisch *et al.* (10). Herein, discussions are focused on the recent development and applications of isomer-resolving MS/MS on deeper structural levels (levels 3–5 in Fig. 1), while more mature techniques for the analysis of lipid class and chain composition are not discussed. The readers can find detailed discussion from the classical reviews (15, 16) and books (17, 18) on these topics.

LIPID CHARACTERIZATION AT THE C=C LOCATION LEVEL

Unsaturated lipids, of which one or more the fatty acyl chains contain at least one C=C, contribute to a significant portion of a lipidome (19). Studies have revealed close relationships between the C=C locations and cell membrane permeability (20), cholesterol-phospholipid interaction (21), and plasticity of cancer cells (22). Bottom-up analysis on total fatty acids via GC-MS is the gold standard for profiling, in which identification of FAs is typically achieved through comparisons to that of the authentic standards. Brenna group developed acetonitrile chemical ionization which allowed for independent structural analysis of unsaturated fatty acid methyl esters (FAMEs) when coupled with collision-induced dissociation (CID) (23, 24). Charge-remote fragmentation (CRF) via high-energy CID, viz. collision energy higher than 1000 eV (lab frame) (25), of the deprotonated FAs, or low-energy CID (collision energy < 200 eV, lab frame) of charge-derivatized FAs produces signature fragmentation pattern around the C=Cs for characterizing unsaturated FAs (26). However, the aforementioned methods cannot be directly applied for probing C=C locations in complex lipids. When the ions of complex lipids are subjected to CID, the most common MS/MS methods installed on commercial MS instruments, cleavage of the nonpolar bonds (C-C or C=C) is energetically unfavorable as

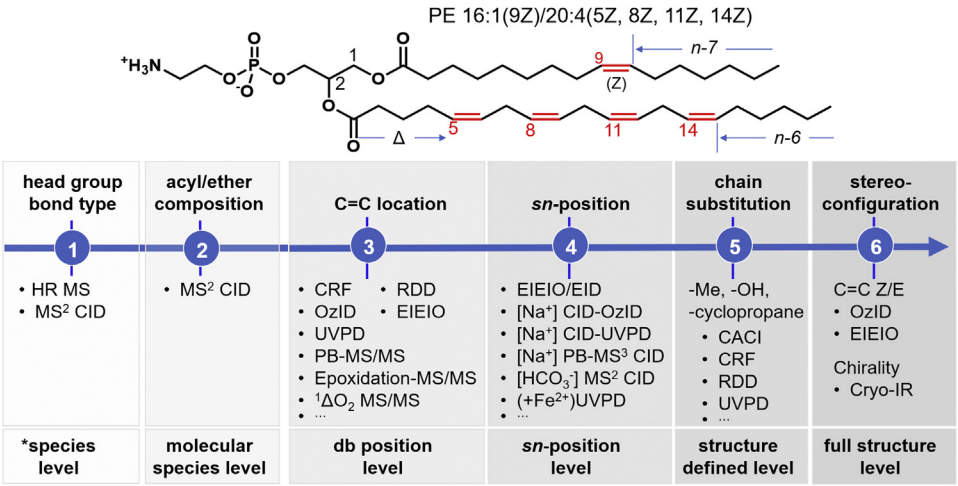

Fig. 1. Structural hierarchy of a complex lipid, represented by a phosphatidylethanolamine molecule: PE 16:1(9Z)/20:4(5Z, 8Z, 11Z, 14Z). The "Δ" and "*n*-" annotations for the locations of C=C are indicated in the structure. The MS/MS methods that have been developed for characterizing at each structural level. *The identified structural levels are named according to Liebisch *et al.* (10)

compared to the polar bonds under charge-directed dissociation, such as ester or phosphoester linkages in complex lipids.

Two approaches have been utilized to characterize the locations of C=C in complex lipids (**Fig. 2**). One involves the development of novel gas-phase ion activation/dissociation methods. These include ozone-induced dissociation (OzID), ultraviolet photodissociation (UVPD), electron impact excitation of ions from organics (EIEIO), metastable atom–activated dissociation (MAD), ion/ion reactions via CRF mechanism, and radical-directed dissociation (RDD). Alternatively, chemical derivatization of C=C to functional groups that can generate informative fragments of C=C locations via CID allows a wider accessibility for labs which do not have access to the specialized instruments. These derivatization methods include the Paternò-Büchi (PB) reaction, epoxidation, and singlet oxygen ($^1\Delta O_2$)-ene reaction. In the following sections, the basic principle of each method for locating C=C is discussed.

GAS-PHASE ION ACTIVATION METHODS FOR LOCATING C=C

Ozone-induced dissociation

Although ozonolysis is highly specific and efficient for cleaving a C=C in lipids, its application for the analysis of complex lipids has been hampered because of the difficulty in linking the identity of the intact lipid to its ozonolysis products when a mixture of unsaturated lipids undergoes ozonolysis altogether. This challenge is overcome by performing gas-phase ozonolysis of mass-isolated lipid ions inside an ion-trapping unit, e.g., a quadrupole ion trap, in a mass spectrometer (27). Following the classic ozonolysis mechanism, the C=C bond is converted into a primary ozonide, which quickly decomposes into an aldehyde ion and a Criegee ion with a constant mass separation of 16 Da. Because of the clear mass relationship between the parent ion (intact lipid) and the two fragments resulting from ozonolysis, the location of C=C in a fatty acyl can be confidently determined (**Scheme 1**a). This technique was pioneered by Blanksby group in 2008 and coined as OzID (27). By coupling with different types of soft ionization methods, OzID has been successfully applied for pinpointing the locations of C=C in various classes of lipids, including FAs, GPLs, GLs, and SLs (28). OzID is also incorporated into data-independent shotgun lipidomics workflow for fast profiling of lipids in human plasma (29). Even though the efficiency of gas-phase ozonolysis is approaching unit efficiency, OzID typically requires seconds of reaction time to accumulate detectable C=C diagnostic fragment ions due to the low number density of ozone allowed in an ion trap (10^9 – 10^{12} molecules cm^{-3}) (27, 30). This aspect reduces the analysis speed and makes its hyphenation with liquid chromatography (LC) inefficient. To circumvent this limitation, Poad *et al.* incorporated OzID in a high-pressure ion-mobility spectrometry (IMS) cell (31), in which the high number density of ozone (~10^{15} molecules cm^{-3}) significantly accelerated ozonolysis, producing abundant C=C fragment ions within 100 ms. High-pressure OzID also facilitates inline coupling with LC separation and its application for identification of a series of C=C location isomers of GPLs. By conducting ozonolysis in a high-pressure trapping ion funnel of an Agilent 6560 IMS QTOF, OzID is further shortened to 10 ms, thus compatible on the time scale of IMS. In this configuration, ozonolysis cannot be conducted on mass-isolated ions; however, the hyphenation with a prior LC and subsequent IMS separations, viz. LC-OzID-IMS-MS, aids in the assignment of ozonolysis products to their associated precursor ions for confident C=C location determination in a nontargeted fashion (32). High-pressure-OzID also greatly improves the acquisition rates (up to 5 pixels s^{-1}) for MALDI-MS/MS imaging of both C=C and *sn*-position isomers in biological tissues, which was recently demonstrated on a SYNAPT HDMS G2-Si Q-TOF mass spectrometer (33).

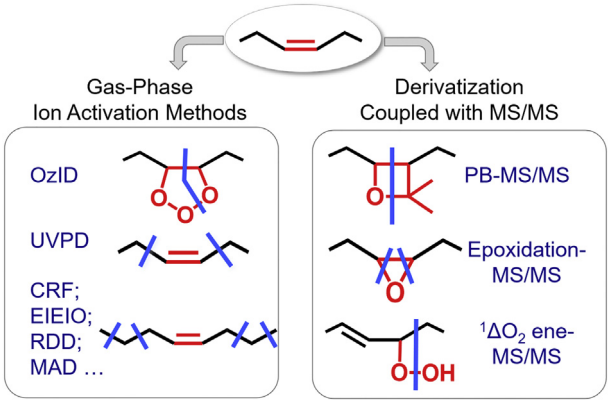

Fig. 2. The two approaches for locating the C=Cs in lipids by MS. The gas-phase ion activation methods, including OzID, UVPD, CRF, EIEIO, RDD, MAD, etc., initiate fragmentation at or around a C=C. Alternatively, the C=C can be firstly transformed into functional groups that are prone to generating informative fragments in subsequent CID. The transformations can be achieved via the PB reaction, epoxidation, and $^1\Delta O_2$-ene reaction. CRF, charge-remote fragmentation; EIEIO, electron impact excitation of ions from organics; MAD, metastable atom–activated dissociation; RDD, radical-directed fragmentation; UVPD, ultraviolet photodissociation.

Ultraviolet photodissociation

Brodbelt and Reid groups independently reported the application of 193 nm UVPD for locating C=Cs in lipids in

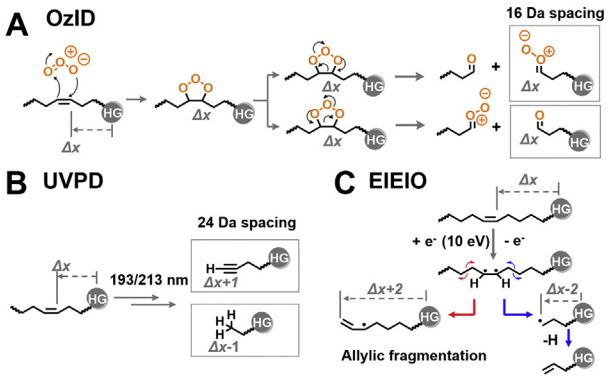

Scheme 1. Gas-phase ion dissociation methods for locating C=C(s) in lipids: (a) OzID, (b) UVPD, and (c) EIEIO. The charge of the ions is carried by the headgroup (HG) and not indicated in the schemes. EIEIO, electron impact excitation of ions from organics; OzID, ozone-induced dissociation; UVPD, ultraviolet photodissociation.

2017 (34, 35). The dissociation is mainly driven by electronic excitation of a C=C due to the absorption of photons of wavelength around 200 nm. This process subsequently initiates cleavages at the vinylic C-C and forms a pair of diagnostic ions with mass difference of 24 Da (Scheme 1b). Although the mechanistic detail is not entirely clear, it is hypothesized that the diradical formed from the photo-excited C=C is responsible for the vinylic cleavages and several other RDD channels (34). The 193 nm UVPD has been implemented in the HCD cell on Orbitrap Elite mass spectrometer and a low-pressure trap on Orbitrap Fusion Lumos mass spectrometer, with 10 laser pulses being used per activation (~20 ms). More recently, 213 nm UVPD, which can be chosen as an add-on module on the Orbitrap mass spectrometers, has been demonstrated for lipid analysis. The 213 nm UVPD shows almost identical fragmentation phenomenon as that of 193 nm UVPD; however, it takes longer time (200 ms) for activation owing to its lower power of the laser source (36). The UVPD methods have been applied to different classes of lipids for locating the C=Cs, such as GPLs (34, 37), cardiolipins (38), FA esters of hydroxy FAs (36), and SLs (35). It has recently been successfully coupled with LC-MS for enhancing quantitation capability for C=C location isomers (39) and with desorption electrospray ionization (DESI) for isomer-resolving imaging (40). A limitation of UVPD for analysis of C=C location is its inherent low fragmentation efficiency due to low photon absorption by a C=C; thus, it often requires a magnification of the spectrum for the detection of diagnostic ions. Using laser source of higher power or incorporating more efficient chromophores in lipids may help improving the sensitivity for characterizing lipids at the C=C location level.

Electron impact excitation of ions from organics

EIEIO or electron-induced dissociation was first developed by Freiser and Cody in 1979 as an alternative dissociation method for singly charged ions (41). This electron-based ion activation concept was adopted for lipid analysis by Baba and Campbell on a modified Q-TOF in 2015 (42) and later by Kane *et al.* on an Fourier transform ion cyclotron resonance (FT-ICR) instrument (43). During EIEIO, positively charged lipid ions are allowed to interact with an electron beam of kinetic energy around 10 eV. Due to electronic excitation of the parent ions, many high-energy and radical-directed dissociation channels are activated. This process produces rich fragmentation in lipids, from which multilevel structural information can be extracted from a single EIEIO spectrum, including the identity of head groups, the location of C=C, the configuration of C=C, *sn*-position, and even the identity of glycans in complex lipids (42, 44–46). This also means that EIEIO is not a fragmentation method specific to C=C. For a saturated fatty acyl chain, EIEIO forms a continuous series of fragment ions differing by CH_2 (14.014 Da) resulting from C-C cleavages along the chain. For an unsaturated fatty acyl chain, the vinylic C-C cleavages and direct C=C cleavages are disfavored relative to the allylic C-C cleavages (Scheme 1c). This difference in relative peak intensities produces a "V" shape fragmentation pattern, which is used for locating a C=C in a fatty acyl chain. However, intrachain fragments generated from the other fatty acyl chains in complex lipids such as in GPLs and GLs may cause interferences and these fragments should be carefully differentiated for confident C=C determination. Computer-assisted spectral interpretation is typically needed for locating C=C from EIEIO (44). Given the complexity of the EIEIO spectra, a prior separation of isobaric or isomeric lipid species is helpful in increasing the confidence for lipid identification. By coupling with differential ion mobility spectrometry for fast lipid species separation, more than 400 lipid molecules including GPLs, GLs, SMs, and glycosphingolipids have been annotated at detailed structural levels from porcine brain lipid extracts (47). The ZenoTOF 7600 mass spectrometer (Sciex, Toronto, Canada) is installed with an EIEIO module, allowing EIEIO to be more accessible for lipid analysis.

Other gas-phase ion activation methods

RDD, CRF, MAD-CID, hydrogen abstraction dissociation, and oxygen attachment dissociation have also been demonstrated for locating the C=Cs in complex lipid structures. These methods rely on accessing radical-directed dissociation or higher energy activation channels to achieve rich fragmentation along fatty acyl chain. The RDD concept for complex lipid analysis was demonstrated by Blanksby group in 2012 (48). In the RDD approach, lipid molecules are derivatized or complexed with a structural moiety containing a photo-labile aryl-iodine. The modified lipids are ionized by ESI as even-electron ions and then subjected to 266 nm UVPD, from which lipid radical ions are uncaged from the homolytic cleavage of C-I in the gas phase. By applying an additional stage of CID to the radical ions, the site of radical is mobilized from the benzyl radical to the methylene groups along the fatty acyl chain due to an almost uniform hydrogen atom transfer. Subsequent RDD induces intrachain cleavages driven by the stability of the product species, from which a characteristic 12 Da spacing of the intrachain fragments is observed for the site of C=C as compared to 14 Da spacing for saturated fatty acyls. This signature is used in the MS^3 PD-CID experiments for locating C=C in unsaturated lipids. It is worth noting that RDD from the allylic position of the C=C is a prominent fragmentation channel directly resulting from 266 nm UVPD of the aryl-iodine derivatized FAs (49), which facilitates the analysis of C=C location isomers in a mixture of 37 FAs implemented on an LC-MS platform (50).

CRF along the fatty acyl chain has been demonstrated for unsaturated FA analysis via high-energy CID of deprotonated anions on sector instruments (51) and later via low-energy CID on metal adduct of FA or fixed-charged derivatized FA cations (26, 52). McLuckey group used charge inversion ion/ion chemistry to synthesize the metal adduct of FA, e.g., the complex cations between fatty acid and phenanthroline magnesium ($[FA\text{-}H+MgPhen]^+$), inside a mass spectrometer; subsequent low-energy CID of the complex triggered CRF along the FA chain, leading to the characteristic "V" pattern around a C=C for unsaturated FAs (53). The same principle was later applied for the structural analysis of GPLs, in which the anions of GPL molecules were firstly fragmented by CID to generate FA anions before going through charge-inversion ion/ion chemistry and subsequent CID steps (54).

Jackson group developed an MS^3 MAD-CID approach, in which the singly charged phosphatidylcholine (PC) cations were firstly converted to the corresponding radical cations by reacting with metastable helium atom (~20 eV), then mass-isolated, and fragmented by low-energy CID (55). The overall fragmentation pattern induced by MAD-CID is similar to that reported by EIEIO. Takahashi *et al.* developed hydrogen abstraction dissociation and oxygen attachment dissociation for the structural analysis of GPLs (56). The interaction between the lipid ions and a neutral hydrogen atom (H•) inside an ion trap induces RDD along the fatty acyl chain. When using OH• and ^3O for the reaction, the C=C is first oxidized and then fragmented at the adjacent methylene bridges,

allowing for the assignment of the C=Cs (56). Due to the requirement of sophisticated MS instrumentation and limited sensitivity, these methods have not yet been applied for large-scale lipid analysis.

C=C SPECIFIC DERIVATIZATION COUPLED WITH MS/MS

Paternò-Büchi-MS/MS

The PB reaction is a [2+2] cycloaddition reaction between an electronically excited ketone or aldehyde and a C=C. The reaction is highly specific to a C=C and can be accomplished in moderate yield (around 30%) within a minute under UV irradiation for a broad range of lipid classes when performed in flow microreactors. Acetone was used as the PB reagent and an ESI solvent in the first demonstration by Ma and Xia in 2014 (57). The reaction was directly performed inside a borosilicate glass emitter of nanoelectrospray ionization (nanoESI) upon irradiation by a 254 nm UV lamp. In such a process, the unsaturated lipids are derivatized online, ionized, and directly subjected to MS analysis. Two regio-PB products (P_1 and P_2) are formed from the cyclization reaction, resulting from two orientations of the addition (**Scheme 2**a). Subsequent MS^2 CID of the mixture of PB products generates a pair of C=C diagnostic fragment ions, one containing an olefin at the cleavage site (F_O) while the other containing an aldehyde (F_A). These ions provide definitive information for pinpointing the locations of the C=Cs. The acetone PB reaction has been incorporated in the shotgun analysis workflow for identification and relative quantitation of FAs and several classes of phospholipids in biological samples (58). It has also been online coupled with LC-MS systems, where a photochemical flow microreactor is connected in between the LC unit and the ESI source. By employing acetone as the mobile phase solvent for hydrophilic interaction chromatography, more than 200 GPLs were identified at the C=C location level from different types of biological samples, including bovine liver extracts, different types of mouse tissue, human plasma, and human breast cancer tissue (59). Improved capability for the identification at the location of C=C level can be achieved for ether versus diacyl GPL isobaric species, chain composition isomers, and C=C *E/Z* isomers by coupling the acetone PB reaction with reversed-phase liquid chromatography (60). It is noted that MS^2 CID of the PB products typically produces more abundant diagnostic ions in positive-ion mode than in negative-ion mode. For anionic GPLs, such as PG and PI, phosphate methylation can be performed prior to PB-MS/MS in positive-ion mode, which improves the limit of identification (LOI, 5 nM for the synthetic standards) (61). Besides, PB-MS/MS has also been incorporated into sampling tip–based devices for the analysis of lipid C=C location isomers in single cells (62).

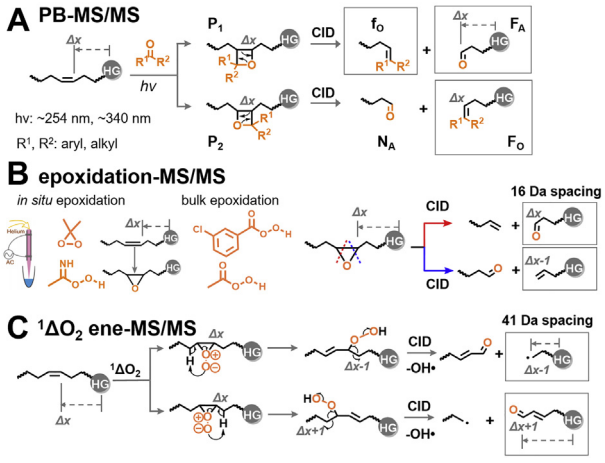

Scheme 2. Double bond–specific derivatization methods coupled with subsequent MS/MS for locating C=C(s) in lipids: (a) the PB reaction, (b) epoxidation, and (c) $^1\Delta O_2$-ene reaction. The charge of the ions is carried by the headgroup (HG) and not indicated in the schemes. PB, Paternò-Büchi.

A series of aryl ketones and aldehydes have been developed besides acetone, rendering flexibility in choosing the most suitable PB reagents for a specific application in lipid analysis (63). For instance, acetyl pyridines (3- and 2-acpy) have been developed as the charge-tagging/charge-switching PB reagents, which improve the LOI for nonpolar lipids including FAs, cholesteryl esters (CEs), and GLs down to the C=C location level (64, 65). By coupling 2-acpy PB reaction with MS^3 or MS^4-CID, the locations of C=Cs can be confidently determined with *sn*-chain specificity for GPLs (66). The high sensitivity of 2-acpy PB-MS/MS further enables single-cell lipidomic analysis at the C=C location level (67).

A very important aspect of the PB reaction is its compatibility with different lipid analysis settings, including MS imaging (MSI) and direct analysis (68, 69). Bednarik *et al.* demonstrated coupling offline on-tissue benzaldehyde PB reaction with MALDI-2-MS/MS (70). Distinct distribution of the Δ 9 versus Δ 11 C=C isomers of PS 18:1_18:1 was revealed in the white and gray areas of mouse cerebellum. By developing PB molecules which could also function as the MALDI matrix, such as benzophenone and 2-benzoylpyridine, Heiles group demonstrated PB derivatization upon 343 nm laser irradiation during the normal MALDI process. Isomer-resolved MS^2 imaging of PCs at the C=C location level is achieved with high lateral resolution (10 μm) in mouse pancreas tissue sections (71).

Epoxidation-MS/MS

Epoxidation converts a C=C to a polar and highly strained three-membered ring. By performing CID on the lipid epoxides, a pair of ions different by 16 Da are formed from ring rupture, which allows for the assignment of C=C location (Scheme 2b). Lipid epoxidation can be achieved by reacting with oxidative species formed in situ in a solution or during nano-ESI

process or with peracids in bulk solution. Zhao *et al.* developed an epoxidation strategy by blowing helium low-temperature plasma (He-LTP) into FAs dissolved in acetone/water solution (72). Almost quantitative conversion of monounsaturated FAs was achieved within one minute. Chemically unstable dioxirane (Scheme 2b) is hypothesized to be the epoxidation reagent. For the analysis of GPLs, acetonitrile is a better solvent for in situ epoxidation via He-LTP, in which peroxycarboximidic acid is likely the oxidant (73). Epoxidation has also been demonstrated via electrochemistry during the process of nano-ESI (74, 75). These in situ epoxidation methods have the advantage of facile and fast analysis of unsaturated lipids.

The classical epoxidation reaction via meta-chloroperoxybenzoic acid was adopted for lipid analysis by Li group (76) and Hsu group (77), independently. Efficient conversion can be achieved for unsaturated FAs (>70%) and GPLs (26%–91%) at room temperature within one hour. The limit of detection of C=C diagnostic ions is at nM range for monounsaturated and polyunsaturated FAs and sub-μ M range for GPLs, the latter of which is mainly limited by performing MS^3 for MS^4 CID in negative-ion mode (77). The aforementioned epoxidation strategy has been integrated with direct fusion ESI, LC-MS, and DESI for imaging lipid C=C location isomers in tissue sections. Very recently, peracetic acid was used as the epoxidation reagent and it was applied for mapping C=C location isomers of FAs in tissues via MALDI-MS/MS (63). Other epoxidation strategies have also been explored; for example, Oxone was used as the epoxidation reagent and applied for the analysis of FA C=C isomers in human plasma samples (78); epoxidation of unsaturated FAs was achieved by pulsed corona discharge generated by triboelectric nanogenerators (79) and by atmospheric pressure chemical ionization (80).

$^1\Delta O_2$-ene reaction

A C=C can be converted to hydroperoxides by reacting with singlet oxygen ($^1\Delta O_2$) existed in ambient air (81) or formed by photosensitizing (82). MS^2 CID of lipid hydroperoxides produces fragments indicative of C=C locations in unsaturated lipids (Scheme 2c). In the report by Laskin group (83), rose bengal dissolved in the ESI or nano-DESI spray solution was used as the photosensitizer, while a green laser pointer (532 nm) was used to initiate the formation of $^1\Delta O_2$. A reaction yield around 30% can be achieved with reaction time estimated shorter than 250 ms. This method has been demonstrated for ambient imaging of lipid isomers via nano-DESI from animal tissue sections.

Characterization at the sn-position level. GPLs and GLs are de novo synthesized and dynamically modified for fatty acyl compositions in the cell (84, 85). These processes generate an array of chain compositional isomers as well as *sn*-isomers. For analysis of GPLs at the *sn*-position level, selective hydrolysis of the ester bond at *sn*-1 or *sn*-2 position via phospholipases A (PLA_1 and PLA_2) followed by LC-MS analysis is the gold standard, albeit of low throughput (86, 87). MS^2 CID of the anions of GPLs typically produces more abundant fragment ions due to neutral loss of the *sn*-2 chain than the *sn*-1 fatty acyl chain; thus, their abundance ratios have been used to differentiate the *sn*-isomers. The ion abundance ratio, however, is dependent on the headgroup, fatty acyl identity, and instrument conditions, rendering a relatively high uncertainty especially for isomer quantitation (88).

The analysis of monoacylglycerides (MAGs) and diacylglycerides (DAGs) can be complicated by facile α-hydroxy acyl migration besides their low endogenous abundances (89). Reports on the analysis of MAGs and DAGs at the *sn*-position level mainly rely on the chemical modification of the free hydroxyl group(s) to reduce acyl migration and produce signature fragmentation patterns for the *sn*-isomers via subsequent MS^2 CID (90, 91). On the other hand, MS^2 CID of the ammonium adduct ions of triacylglycerols (TAGs) forms abundant DAG product ions, which is widely used for identification of GLs at the fatty acyl composition level (92). It is observed that the neutral loss of fatty acyls as free FAs from *sn*-1/3 positions are more favorable than the *sn*-2 position. However, the abundance ratios of these DAG product ions are also dependent on the FA compositions, especially at the presence of PUFA, making this method less rigorous for differentiating *sn*-isomers (93). Hsu and Turk showed that further CID of the DAG ions improved differentiation among positional isomers due to an exclusive loss of the *sn*-2 chain as an *α,β*-unsaturated FA (94). However, nonlinear effects exist, thus complicating its application for the analysis of complex TAG mixtures.

In a mechanistic study conducted by Hsu and Turk, they proved that the C_α-H on fatty acyl chains instead of the C_2-H on glycerol backbone participated in the phospho-head group loss (HOE loss in **Scheme 3**a) from CID of PC cations ($[M + H/Li]^+$) (95). A preference to removing the C_α-H on *sn*-2 over *sn*-1 chain forms a dioxolane ring in the product ions (structure shown in Scheme 3a). This mechanistic insight facilitates the development of a suite of new MS/MS methods for analysis of the *sn*-isomers of GPLs and GLs. For instance, noticing that the proposed fragment structure contains a newly formed C=C between C1 and C2 of the fatty acyl chain, Blanksby group conducted MS^3 CID-OzID experiments on GPLs ($[M + Na]^+$) and proved the formation of the dioxolane-type products as the dominant pathway (96), the structure of which was recently corroborated by cryogenic infrared spectroscopy measurements (97). More importantly, OzID of the newly formed C=C in the dioxolane-type products provides fragment ions only containing the *sn*-1 chain information, allowing definitive assignment of the *sn*-

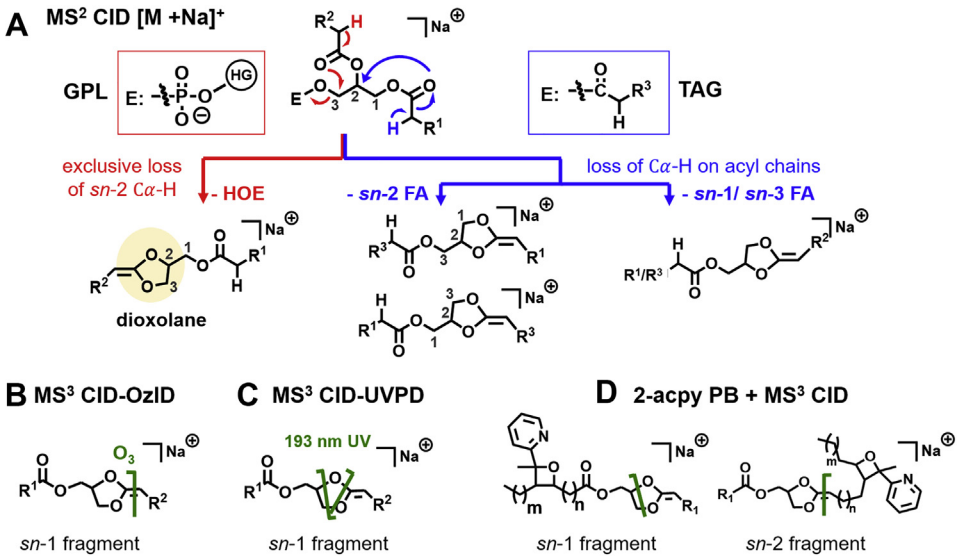

Scheme 3. The MS/MS methods capable of analyzing GPLs and TAGs at the *sn*-position level. (a) Formation of a dioxolane-type fragment ion from MS^2 CID of $[M + Na]^+$ of GPLs. Loss of the *sn*-2 C α-H is the exclusive pathway involved in the phospho-headgroup loss (-HOE) from $MS^{2/3}$ CID of protonated or metal adduct of GPLs. The dioxolane-type fragment ion contains a C=C newly formed between the first two carbons of the *sn*-2 acyl chain. For TAGs, the C α-H can be lost from any of the three *sn*-positions, and thus, four structures of dioxolane-type fragment ions are formed if the three chains have different masses. (b) MS^3 CID-OzID, (c) MS^3 CID-UVPD, and (d) 2-acpy PB coupled with MS^3 CID for analysis of *sn*-isomer of GLPs. GPL, glycerophospholipid; CID, collision-induced dissociation; OzID, ozone-induced dissociation; UVPD, ultraviolet photodissociation; PB, Paternò-Büchi.

geometry in GPLs (Scheme 3b). The relative ion abundances of the OzID products can be used to achieve relative quantitation of *sn*-isomers of GPLs, which are of great value especially when the isomers cannot be chromatographically separated (98).

Targeting the unique C=C formed in the dioxolane-type fragment ions, 193 nm UVPD was incorporated in an MS^3 CID-UVPD sequence for the assignment of *sn*-position isomers of GPLs ($[M + Na]^+$) (34). UVPD cleaves multiple bonds of the five-membered dioxolane ring, producing more diverse product ions than the CID-OzID approach (Scheme 3c). MS^2 CID of the 2-acpy PB products of GPLs ($[M + Na]^+$) is also capable of forming the dioxolane-type fragment ions. By conducting a further stage of CID, *sn*-specific product ions can be obtained (Scheme 3d). Using 2-acpy, the PB-MS^3 CID method allows for identification of the C=C locations and *sn*-positions in the same mass spectrum. Interestingly, the conventional PB reagents such as acetone and benzophenone do not produce abundant dioxolane-type product ions via CID, while the 2-acpy PB products provide about ~20-fold enhancement of the dioxolane-type product ions (66).

Although the dioxolane-type fragments are also formed from the neutral loss of FA via MS^2 CID of TAG ($[M + Na]^+$), the analysis of a mixture of TAG *sn*-isomers turns out to be more challenging. This is because MS^2 CID of each *sn*-pure TAG can produce four dioxolane-type fragments if the three chains are different in mass (Scheme 3a). Further application of OzID/UVPD on these dioxolane product ions will generate FA fragment ions with overlapping *m/z* to those from the *sn*-isomers, making independent identification difficult. A combination of *sn*-resolving separation techniques with these MS/MS methods is most suitable for the identification and quantitation of TAG *sn*-isomers (99).

EIEIO is capable of pinpointing *sn*-isomers of GPLs and TAGs without a need for isomer separation. Upon EIEIO, the fragment peaks resulting from the loss of two fatty acyl chains are diagnostic to the assignment of *sn*-positions for TAGs (**Scheme 4**a). The combined loss of the *sn*-1(or *sn*-3) and *sn*-2 fatty acyl chains leads to the formation of a doublet with 2 Da difference in mass, signature for fatty acyl located at either *sn*-1 or *sn*-3. The fragmentation scheme for the formation of *sn*-1 fragments is shown as an example in Scheme 4a. On the other hand, the double loss of *sn*-1 and *sn*-3 fatty acyls forms the *sn*-2 fragment ions as a singlet. For GPLs, EIEIO can induce a cleavage between C1-C2 in the glycerol backbone, forming a distinct *sn*-2 fragment ion for the *sn*-position assignment (Scheme 4b) (42). Baba *et al.* coupled DMS with EIEIO and demonstrated detailed structural analysis of over 300 lipids together with relative quantitation of the *sn*-isomers of some GPLs and GLs (47).

The phosphocholine head group establishes strong hydrogen bonding with bicarbonate anion (HCO_3^-). MS^2 CID of this complex ($[M + HCO_3]^-$) induces a homolytic C-N cleavage within the choline moiety and generates the carbon-centered radical anions which further dissociate to from the *sn*-1 fragment (Scheme 4c). Based on this RDD pathway, Zhao *et al.* established an LC-MS/MS workflow for identification and quantitation of the *sn*-isomers of PCs (100) and

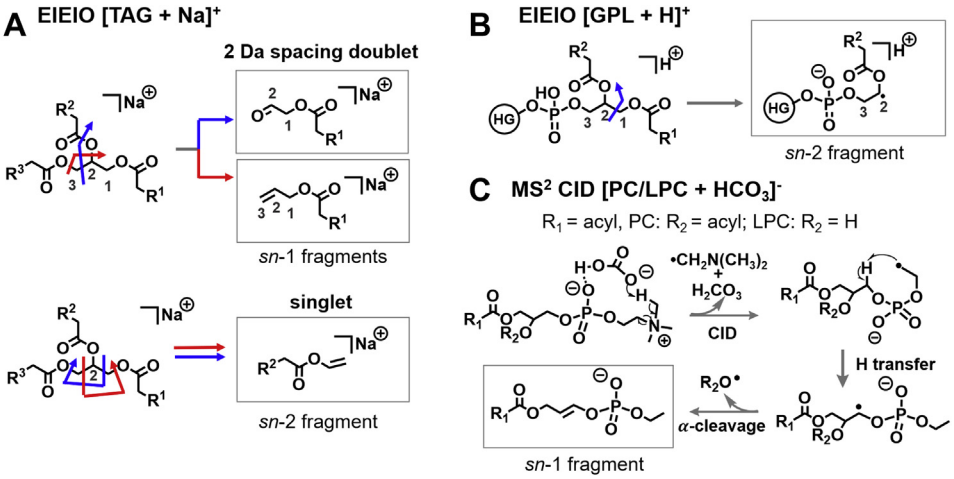

Scheme 4. (a) Formation of the *sn*-specific fragment ions from EIEIO of TAG ($[M+Na]^+$). The doublet with 2 Da mass difference is a signature for *sn*-1 or *sn*-3 fragments while *sn*-2 fragment appears as a singlet. (b) Formation of the *sn*-2 fragment from EIEIO of GPL ($[M + H]^+$). (c) Formation of the *sn*-1 fragment via MS^2 CID of PC or LPC ($[M + HCO_3]^-$). EIEIO, electron impact excitation of ions from organics; CID, collision-induced dissociation; GPL, glycerophospholipid.

lysophosphatidylcholines (LPCs) in lipid extracts (101). In another report, Heiles group showed that 213 nm UVPD of PC ($[M + Fe]^{2+}$) produced signature fragment ions for the assignment of *sn*-isomers of PCs from lipid extracts (102).

Characterization of chain modifications. Methyl branched-chain fatty acids (BCFAs) are abundant in bacteria, skin secretions, rumen tissue, and milk (103). Brenna group has developed EI-MS^2 CID (104) and covalent adduct chemical ionization-MS^2 CID for structural elucidation and quantitation of the methyl esters of BCFAs (105, 106). These methods enabled the discovery of fatty acid desaturase 2 (FADS2) as the desaturase for BCFAs and odd-chain saturated fatty acids (107). Cyclopropane modification is commonly found in various gram-positive and gram-negative bacteria (108). This modification is catalyzed by cyclopropane FA synthase in which process a methylene group derived from S-adenosylmethionine is inserted to a C=C (109). The cyclopropane group has a weak absorption around the wavelength of 200 nm and can be dissociated by 193 nm or 213 nm UVPD via dual cross-ring C–C cleavages on both sides of the cyclopropane ring. The diagnostic ions are mass separated by 14 Da, different from UVPD of a C=C, thus enabling the rule for identification and localization of cyclopropane on a fatty acyl chain. Brodbelt group integrated 213 nm UVPD with LC-MS/MS and identified a series of cyclopropyl GLPs in *Escherichia coli* (*E. coli*) and mycolic acids in *Mycobacterium bovis (M. bovis)* and *Mycobacterium tuberculosis* lipid extracts (110).

CRF and RDD are both capable of inducing C-C cleavages along fatty acyl chain. This unique aspect has been utilized to characterize various chain modifications. Han group demonstrated that the distinct MS^2 CID fragmentation patterns of chain modification isomers were generated from fixed-charge derivatization of FAs. The types of modifications being evaluated include nitrosylation, hydroxylation, and methyl branching (26). Blanksby group and Julian group applied RDD for the analysis of chain modifications via UVPD of C-I bond in covalently modified lipids (50) or lipids noncovalently complexed with a photocaged radical initiator (48). One common feature of these derivatization reagents is that they all contain a photolabile aryl-iodide motif, which can liberate an aryl radical upon 266 nm UVPD at high efficiency. Acyl chain modifications include methyl branching, cyclopropane modification, and hydroxylation on FAs can be identified and localized from performing MS^3 UVPD-CID. By employing a new generation of photocaged radical initiator, 1-(3-(aminomethyl)-4-iodophenyl)pyridin-1-ium, Blanksby group found that 266 nm UVPD was efficient in producing direct photolysis of C-C bonds adjacent to the hydroxyl group (111). Additionally, RDD produces a distinctive 29 Da spacing for simple hydroxyl fatty acids derivatized by 1-(3-(aminomethyl)-4-iodophenyl)pyridin-1-ium, while a 30 Da spacing was observed for polyunsaturated hydroxyl fatty acids, e.g., isomers from the hydroxyeicosatetraenoic acid and hydroxyeicosapentaenoic acid families. This method is compatible with LC-MS analysis time and has a potential to be employed for identification of chain-modified FAs in biological matrices.

The RDD approach via CID of the $[M + HCO_3]^-$ (M: PC, LPC, SM) has been utilized for the characterization of chain modifications (101). By integrating on an LC-MS system, the iso- and anteiso-branched LPC 17:0 isomers have been identified and relatively quantified (101). In another report, C-2 hydroxylation of N-acyls and iso-methyl branched sphingosine base were identified from SMs of *C. elegans* (112). The intrachain fragments generated from these methods are of

relatively low ion abundances, thus limiting the sensitivity of this method.

Quantitation of lipid isomers. Given that lipid isomers are derived from distinct biosynthetic pathways, quantitation of lipids at various isomeric levels is important to deepen the understanding of lipid metabolism. For situations where the isomers can be well resolved by separations and the synthetic standards are available, isomer quantitation is straightforward by constructing the calibration curve from their synthetic standards. The aforementioned situation, however, is rarely encountered, especially for complex lipids. Most synthetic standards of the lipid isomers are not available and they cannot be separated under typical separation conditions used in large-scale lipid profiling. Under these circumstances, isomer-resolving MS/MS methods as discussed in previous sections are instrumental in providing quantitation of lipid isomers. For instance, a linear calibration curve can be obtained by plotting the abundance ratios of the diagnostic ions as a function of the molar ratios of the isomers when the synthetic standards of the isomers are available, however, not resolved by separations (**Fig. 3**A). The molar fraction of the isomers from an unknown can thus be extracted from the calibration curve (Fig. 3B). When the total quantity of the isomer is known, the concentration information can be further obtained. Examples of isomer quantitation following this principle have been shown for both C=C location isomers and *sn*-isomers (58, 65). When the standards are not available, only "relative fractional quantitation" can be obtained because how the structural differences of the isomers might affect ionization and fragmentation is unknown. In this case, the abundance ratios or fractions of the diagnostic ions are directly used for relative fractional quantitation. Relative fractional quantitation is a useful readout for monitoring dysregulated lipid metabolism in various applications as discussed in the later section. Isomer quantitation has also been performed using a certain pattern of the fragment ions when diagnostic ions are not formed, in which more complex calibrations are involved (26, 47, 113).

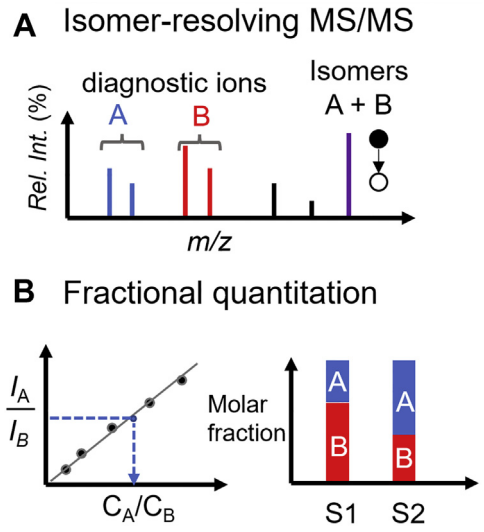

Fig. 3. Schematics for isomer quantitation by isomer-resolving MS/MS: (A) forming diagnostic fragment ions for each isomer (A, B) by MS/MS and (B) constructing a calibration curve and obtaining molar fraction of each isomer if the synthetic standards are available for different biological samples (S1 and S2). If synthetic standards are not available, "relative fractional quantitation" is achieved from measuring the abundance ratios of the diagnostic ions (I_A/I_B).

APPLICATIONS OF DETAILED LIPID STRUCTURAL ANALYSIS

In recently years, the isomer-resolving MS/MS methods are increasingly applied for identification and quantitation of complex lipids at the levels of C=C location and *sn*-position as summarized in Table 1. These types of detailed information provide direct evidence to studying the metabolism of lipid isomers. Young *et al.* used OzID-MS/MS to investigate substrate promiscuity of the human FADS2 (116). In combination with gene silencing and stable isotope tracing, FADS2 was found to promote the production of n-8, n-10, and n-12 lipid species that have rarely been reported previously in human cell lines (**Fig. 4**A). The distribution of lipid isomers in tumor microenvironment was further revealed by MALDI-OzID-MS/MS imaging, suggesting distinct enzyme-substrate interactions in tumor regions. In another report, Li *et al.* studied the response of cellular lipidome under SCD1 inhibition at the single-cell level (67). The relative amounts of lipid C=C location isomers in MDA-Mb-468 cell lines were found to change significantly after SCD1 inhibition by CAY10566 (Fig. 4B). The abundances of PCs containing the n-7 isomers of C16:1 and C18:1 decreased significantly upon inhibition, while the abundances of PCs containing C18:2 (n-6, n-9) and the n-10 isomers of C16:1 and C18:1 increased (Fig. 4C). This may result from an enhanced FADS2 activity due to the inhibition of SCD1.

Mammalian C18:1 typically consists of n-9 (or Δ9) and n-7 (or Δ11) as the two major C=C location isomers resulting from distinct biosynthetic pathways (Fig. 4D). The relative abundance of the isomers can be affected due to a dysregulated lipid metabolism caused by the unset or progression of disease. For instance, the relative compositions of the n-9 and n-7 isomers of C18:1 in a variety of PCs and PEs were found to change significantly between plasma samples of normal control and type 2 diabetes (T2D) patients and tissue samples from breast cancer patients using an LC-PB-MS/MS method (59). In combination with methylation and charge tagging, PB-MS/MS also enabled sensitive screening of potential plasma lipid C=C isomer biomarkers of T2D in other classes of lipids such as anionic GPLs (61), FAs

TABLE 1. A list of MS/MS approaches for characterization of complex lipids at the levels of C=C location and *sn*-position

Structure Information	MS Approach	Lipids	Samples	Reference
C=C locations	Shotgun PB-MS/MS	FA and GPL	Lipid extracts	(58)
	LC-PB-MS/MS	FA and GPL	Lipid extracts, plasma samples	(59–61, 65)
	MALDI-PB-MS/MS	GPL and glycosphingolipid,	Mouse brain tissue	(70, 114)
	UVPD-MS	PC, cardiolipin, FA, sphingolipid, SM, TG	*E. coli* and human papillary thyroid carcinoma extracts	(35, 36, 38, 115)
	LC-UVPD-MS	FA and GPL	Bovine liver and porcine brain extracts	(49, 63)
	DESI-UVPD-MS	PC	Brain tissue, lymph node tissue	(40)
	OzID-MS	GPL, SM, TG	Lipid extracts	(27, 31)
	LC-OzID-MS	PC, PE, SM	Human plasma	(32)
	epoxidation-MS/MS	FA and GPL	Bovine liver extract, human plasma, yeast extract, serum samples	(63, 72, 73, 76)
	epoxidation-LC-MS/MS	FA and GPL	Human serum	(76)
	epoxidation-DESI-MS/MS	FA and GPL	Human serum, mouse adipocytes, and cancer tissue sections	(76)
	epoxidation-MALDI-MS/MS	FA	Cancer tissue samples, human cell lines	(63)
	HAD/OAD- MS/MS	PC and LPC	Standards	(56)
sn-positions	$(+Na^+)$ PB-MS^3	GPL	Human breast cancer cells	(66)
	$(+Na^+)$ OzID-MS^3	GPL	Cow brain and kidney extracts	(96, 98)
	$(+Na^+)$ UVPD-MS^3	GP	Bovine liver and porcine brain extracts	(34)
	$(+HCO_3^-)$ PB-MS^3	PC	Tissue samples of human breast cancer	(100)
	$(+Fe^{2+})$ UVPD-MS^3	PC	Lipid extracts of mouse pancreas tissue	(102)
	EIEIO	PC	Egg yolk extracts	(42)

FA, fatty acid; GPL, glycerophospholipid; TG, triglyceride; EIEIO, electron impact excitation of ions from organics; UVPD, ultraviolet photodissociation; OzID, ozone-induced dissociation; OAD, oxygen attachment dissociation; PB, Paternò-Büchi.

(65), DAGs, and TAGs (117). By discrimination of both C=C and *sn*-isomers of GPLs, it showed further advantage in phenotyping different disease states and discovery of differentiating lipids (66). For example, no statistically significant change was obtained by using either relative abundance of C=C location isomers or *sn*-position isomers of certain GPLs for the discrimination of non-small cell lung cancer tissues from adjacent normal tissues. However, using information from both C=C and *sn*-isomers from a series of GPLs, all the tissues were correctly classified by hierarchical cluster analysis.

Paine *et al.* applied MALDI-OzID-MSI for the analysis of medulloblastoma tumor in mouse brain tissue samples (33, 118). Altered isomeric populations in the tumor were observed relative to the surrounding white and gray matter, such as the *sn*-isomers of PC 16:0_18:1, PC 18:0_18:1, and PC 16:0_20:1, and the n-7 C=C location

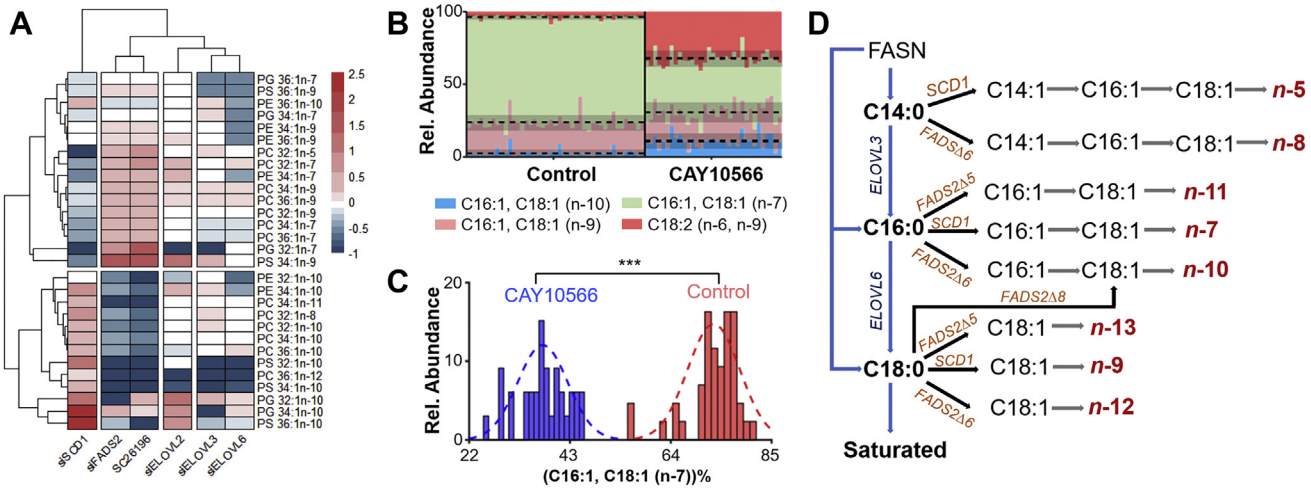

Fig. 4. A: Heatmap of the C=C location isomers of GPLs in treated LNCaP cells relative to untreated cells (116), showing that SCD1-related lipids (the n-7 and n-9 isomers) and FADS2-related lipids (the n-10 isomers) have inversed abundance shifts due to silencing of SCD1 and FADS2, respectively. (Reprinted with permission (116). Copyright 2021 Elsevier). B: Alterations in the relative amounts of the C=C location isomers of PC 34:2 in MDA-MB-468 single cells upon SCD1 inhibition (67) and C) significant decrease of the C16:1(n-7) and C18:1(n-7) isomers of PC 34:2. (Reprinted with permission (67). Copyright 2021 Springer Nature). D: Synthetic pathways of different C=C location isomers of monounsaturated FAs in human cells (modified from (116)). FADS2, fatty acid desaturase 2; GPL, glycerophospholipid.

isomers in PC 34:1 and PC 36:1. Marshall *et al.* incorporated OzID into data-independent shotgun lipidomics workflow for two-dimensional characterization of lipid isomers in human plasma (29). It revealed that most unsaturated lipids were present as isomeric mixtures, some of which showed common origins in lipid biosynthesis, indicating that human plasma lipidome may be a valuable resource to unresolved new lipid isomers biomarkers. In a recent report, significant alterations in n-10/n-9 ratios of lipids in human prostate tissues were demonstrated, including PS 34:1, PS 36:1, PE 36:1, and PC 34:1 (116). Klein *et al.* coupled DESI with UVPD for imaging C=C location isomers in tissue samples (40). For human lymph node tissue containing thyroid cancer metastasis, the intensity ratios of PC 16:0_18:1(n-9) to PC 16:0_18:1(n-7) showed different distributions between normal and cancerous portions of the tissue. DESI-UVPD-MSI allowed the discrimination of breast cancer subtypes of different hormone receptor status based on the relative abundances of the n-9 and n-7 isomers of FA 18:1 (119). DESI-MSI via a prior metachloroperoxybenzoic acid epoxidation revealed significant increase of PG 16:0_18:1(n-7) isomer in the tumor cell regions (77). Using peracetic acid for epoxidation, a MALDI-MSI approach was recently reported, which showed high sensitivity for imaging the C=C location isomers of FAs in murine melanoma tumor (63).

CONCLUSIONS AND OUTLOOK

We have seen a rapid expansion of MS/MS methods capable of resolving lipid isomers at various structural levels over the past few years. These developments lead to the discovery of novel lipid molecules, show the possibility to untangle lipid metabolism involving isomers, and offer a new direction for biomarker discovery. While promising, many of the techniques are in the early stage of development; further technical advancement is needed for them to evolve as the tool of choice for lipid profiling in the future. For instance, most methods work better in positive-ion mode regarding formation of the diagnostic fragment ions, which thus have limited sensitivity for anionic lipids (e.g., PA and PI) and nonpolar lipids (e.g., FA, GL, and CE). Some successes have been achieved by enhancing ionization of these lipid classes in positive-ion mode via phosphate methylation or charge tagging. Nevertheless, isomer-resolving MS/MS methods which are independent of the charge polarity of lipids need to be explored. It is also desirable to integrate isomer-resolving MS/MS methods with different lipidomic analysis workflows, especially LC-MS, one of the major platforms for lipid analysis. This requires innovations in instrumentation to shorten the ion activation time of MS/MS to tens of ms while still producing abundant diagnostic fragment ions so that they can be compatible with LC separations. With new developments in methodologies and instrumentation, IMS has gained increasing attention in MS applications during the past few years (120). IMS provides a dimension of separation according to the collision cross sections of lipid ions in tens of milliseconds timescale (121), which is readily compatible with shotgun analysis, LC separations, MS imaging, and isomer-resolving MS/MS on several commercial mass spectrometers. While there are solutions for locating C=C or *sn*-position in lipids as emphasized in this review, new MS methods, likely through an integration with gas-phase spectroscopy, such as cryo-infrared spectroscopy (122), are needed to solve more challenging structural problems, including stereo-configuration of the C=C and the identity of the glycans.

There is always a trade-off between sensitivity and the level of structural information one can get. For the MS methods discussed herein, they typically offer an LOI in the range of nM to sub-μM, one to two orders of magnitude higher than the measurements without differentiating lipid isomers. To push detailed structural analysis to the lipids of lower abundances, such as lipid mediators or single-cell lipidome, integration with pre-enrichment methods will help in this regard. With the new capabilities of deep-lipidotyping, of equal importance is development of tools for data analysis and automated lipid annotation at deeper structural levels (123). This development is critical to speeding up the transfer of new MS methods from expert labs to ordinary lipid analysis labs.

Due to the shortage of the lipid standards, it remains challenging for quantitation of complex lipids in biological samples. Relative quantitation of lipid isomers thus provides a simple and effective means to study the change of lipids from different biological states. Several examples have shown that relative quantitation of C=C location isomers or *sn*-position isomers is more sensitive in the discovery of differentiating lipids which might be potential biomarkers. It is expected that more lipidomics labs will be interested in using deep-lipidotyping as a new means to investigate lipid functions and metabolism.

Author contributions

W. Z. and Y. X. wrote the manuscript. R. J., J. Z., and Y. L. prepared the figures. All authors critically reviewed the article.

Author ORCIDs

Yu Xia https://orcid.org/0000-0001-8694-9900

Funding and additional information

This work was supported by the National Key R&D Program of China (2018YFA0800903) and National Natural Science Foundation of China (No. 22074075).

Conflict of interest

The authors declare that they have no known competing financial interests or personal relationships that could have appeared to influence the work reported in this paper.

Abbreviations

BCFA, branched-chain fatty acid; CID, collision-induced dissociation; CRF, charge-remote fragmentation; EIEIO, electron impact excitation of ions from organics; FADS2, fatty acid desaturase 2; GL, glycerolipid; GPL, glycerophospholipid; IMS, ion-mobility spectrometry; MAD, metastable atom–activated dissociation; OzID, ozone-induced dissociation; PB, Paternò-Büchi; RDD, radical-directed fragmentation; SL, sphingolipid; UVPD, ultraviolet photodissociation.

Manuscript received March 16, 2022, and in revised from April 19, 2022. Published, JLR Papers in Press, April 27, 2022, https://doi.org/10.1016/j.jlr.2022.100219

REFERENCES

1. Han, X., and Gross, R. W. (2003) Global analyses of cellular lipidomes directly from crude extracts of biological samples by ESI mass spectrometry: a bridge to lipidomics. *J. Lipid Res.* **44**, 1071–1079
2. Wenk, M. R. (2005) The emerging field of lipidomics. *Nat. Rev. Drug Discov.* **4**, 594–610
3. Wenk, M. R. (2010) Lipidomics: New Tools and Applications. *Cell.* **143**, 888–895
4. Lam, S. M., Zhang, C., Wang, Z., Ni, Z., Zhang, S., Yang, S., *et al.* (2021) A multi-omics investigation of the composition and function of extracellular vesicles along the temporal trajectory of COVID-19. *Nat. Metab.* **3**, 909–922
5. Lipidomics Standards Initiative, C. (2019) Lipidomics needs more standardization. *Nat. Metab.* **1**, 745–747
6. Currie, E., Schulze, A., Zechner, R., Walther, T. C., and Farese, R., Jr. (2013) Cellular fatty acid metabolism and cancer. *Cell Metab.* **18**, 153–161
7. Quehenberger, O., Armando, A. M., and Dennis, E. A. (2011) High sensitivity quantitative lipidomics analysis of fatty acids in biological samples by gas chromatography-mass spectrometry. *Biochim. Biophys. Acta.* **1811**, 648–656
8. Schwudke, D., Hannich, J. T., Surendranath, V., Grimard, V., Moehring, T., Burton, L., *et al.* (2007) Top-down lipidomic screens by multivariate analysis of high-resolution survey mass spectra. *Anal. Chem.* **79**, 4083–4093
9. Züllig, T., Trötzmüller, M., and Köfeler, H. C. (2020) Lipidomics from sample preparation to data analysis: a primer. *Anal. Bioanal. Chem.* **412**, 2191–2209
10. Liebisch, G., Fahy, E., Aoki, J., Dennis, E. A., Durand, T., Ejsing, C. S., *et al.* (2020) Update on LIPID MAPS classification, nomenclature, and shorthand notation for MS-derived lipid structures. *J. Lipid. Res.* **61**, 1539–1555
11. Voinov, V. G., Bennett, S. E., Beckman, J. S., and Barofsky, D. F. (2014) ECD of tyrosine phosphorylation in a triple quadrupole mass spectrometer with a radio-frequency-free electromagnetostatic cell. *J. Am. Soc. Mass Spectrom.* **25**, 1730–1738
12. Chi, A., Huttenhower, C., Geer, L. Y., Coon, J. J., Syka, J. E., Bai, D. L., *et al.* (2007) Analysis of phosphorylation sites on proteins from Saccharomyces cerevisiae by electron transfer dissociation (ETD) mass spectrometry. *Proc. Natl. Acad. Sci. U. S. A.* **104**, 2193–2198
13. Wolff, J. J., Laremore, T. N., Aslam, H., Linhardt, R. J., and Amster, I. J. (2008) Electron-induced dissociation of glycosaminoglycan tetrasaccharides. *J. Am. Soc. Mass Spectrom.* **19**, 1449–1458
14. Porta Siegel, T., Ekroos, K., and Ellis, S. R. (2019) Reshaping lipid biochemistry by pushing barriers in structural lipidomics. *Angew. Chem. Int. Ed.* **58**, 6492–6501
15. Han, X. (2016) Lipidomics for studying metabolism. *Nat. Rev. Endocrinol.* **12**, 668–679
16. Yang, K., and Han, X. (2016) Lipidomics: techniques, applications, and outcomes related to biomedical sciences. *Trends Biochem. Sci.* **41**, 954–969
17. Murphy, R. C. (2014) Tandem Mass Spectrometry of Lipids: Molecular Analysis of Complex Lipids. Royal Society of Chemistry, London, UK
18. Han, X. (2016) Lipidomics: Comprehensive Mass Spectrometry of Lipids. John Wiley & Sons, NJ
19. Lorent, J. H., Levental, K. R., Ganesan, L., Rivera-Longsworth, G., Sezgin, E., Doktorova, M., *et al.* (2020) Plasma membranes are asymmetric in lipid unsaturation, packing and protein shape. *Nat. Chem. Biol.* **16**, 644–652
20. Subbaiah, P. V., Sircar, D., Aizezi, B., and Mintzer, E. (2010) Differential effects of conjugated linoleic acid isomers on the biophysical and biochemical properties of model membranes. *Biochim. Biophys. Acta.* **1798**, 506–514
21. Martinez-Seara, H., Róg, T., Pasenkiewicz-Gierula, M., Vattulainen, I., Karttunen, M., and Reigada, R. (2008) Interplay of unsaturated phospholipids and cholesterol in membranes: effect of the double-bond position. *Biophys. J.* **95**, 3295–3305
22. Vriens, K., Christen, S., Parik, S., Broekaert, D., Yoshinaga, K., Talebi, A., *et al.* (2019) Evidence for an alternative fatty acid desaturation pathway increasing cancer plasticity. *Nature.* **566**, 403–406
23. Lawrence, P., and Brenna, J. T. (2006) Acetonitrile covalent adduct chemical ionization mass spectrometry for double bond localization in non-methylene-interrupted polyene fatty acid methyl esters. *Anal. Chem.* **78**, 1312–1317
24. Wang, D. H., Wang, Z., Cortright, J. R., Le, K. P., Liu, L., Kothapalli, K. S. D., *et al.* (2020) Identification of polymethylene-interrupted polyunsaturated fatty acids (PMI-PUFA) by solvent-mediated covalent adduct chemical ionization triple quadrupole tandem mass spectrometry. *Anal. Chem.* **92**, 8209–8217
25. Griffiths, W. J. (2003) Tandem mass spectrometry in the study of fatty acids, bile acids, and steroids. *Mass Spectrom. Rev.* **22**, 81–152
26. Wang, M., Han, R. H., and Han, X. (2013) Fatty acidomics: global analysis of lipid species containing a carboxyl group with a charge-remote fragmentation-assisted approach. *Anal. Chem.* **85**, 9312–9320
27. Thomas, M. C., Mitchell, T. W., Harman, D. G., Deeley, J. M., Nealon, J. R., and Blanksby, S. J. (2008) Ozone-induced dissociation: elucidation of double bond position within mass-selected lipid ions. *Anal. Chem.* **80**, 303–311
28. Brown, S. H., Mitchell, T. W., and Blanksby, S. J. (2011) Analysis of unsaturated lipids by ozone-induced dissociation. *Biochim. Biophys. Acta.* **1811**, 807–817
29. Marshall, D. L., Criscuolo, A., Young, R. S. E., Poad, B. L. J., Zeller, M., Reid, G. E., *et al.* (2019) Mapping unsaturation in human plasma lipids by data-independent ozone-induced dissociation. *J. Am. Soc. Mass Spectrom.* **30**, 1621–1630
30. Poad, B. L., Pham, H. T., Thomas, M. C., Nealon, J. R., Campbell, J. L., Mitchell, T. W., *et al.* (2010) Ozone-induced dissociation on a modified tandem linear ion-trap: observations of different reactivity for isomeric lipids. *J. Am. Soc. Mass Spectrom.* **21**, 1989–1999
31. Poad, B. L. J., Green, M. R., Kirk, J. M., Tomczyk, N., Mitchell, T. W., and Blanksby, S. J. (2017) High-pressure ozone-induced dissociation for lipid structure elucidation on fast chromatographic timescales. *Anal. Chem.* **89**, 4223–4229
32. Poad, B. L. J., Zheng, X., Mitchell, T. W., Smith, R. D., Baker, E. S., and Blanksby, S. J. (2018) Online ozonolysis combined with ion mobility-mass spectrometry provides a new platform for lipid isomer analyses. *Anal. Chem.* **90**, 1292–1300
33. Claes, B. S. R., Bowman, A. P., Poad, B. L. J., Young, R. S. E., Heeren, R. M. A., Blanksby, S. J., *et al.* (2021) Mass spectrometry imaging of lipids with isomer resolution using high-pressure ozone-induced dissociation. *Anal. Chem.* **93**, 9826–9834
34. Williams, P. E., Klein, D. R., Greer, S. M., and Brodbelt, J. S. (2017) Pinpointing double bond and sn-positions in glycerophospholipids via hybrid 193 nm ultraviolet photodissociation (UVPD) mass spectrometry. *J. Am. Chem. Soc.* **139**, 15681–15690
35. Ryan, E., Nguyen, C. Q. N., Shiea, C., and Reid, G. E. (2017) Detailed structural characterization of sphingolipids via 193 nm ultraviolet photodissociation and ultra high resolution tandem mass spectrometry. *J. Am. Soc. Mass Spectrom.* **28**, 1406–1419
36. Buenger, E. W., and Reid, G. E. (2020) Shedding light on isomeric FAHFA lipid structures using 213 nm ultraviolet photodissociation mass spectrometry. *Eur. J. Mass. Spectrom.* **26**, 311–323
37. Klein, D. R., Blevins, M. S., Macias, L. A., Douglass, M. V., Trent, M. S., and Brodbelt, J. S. (2020) Localization of double bonds in

bacterial glycerophospholipids using 193 nm ultraviolet photodissociation in the negative Mode. *Anal. Chem.* **92**, 5986–5993
38. Macias, L. A., Feider, C. L., Eberlin, L. S., and Brodbelt, J. S. (2019) Hybrid 193 nm Ultraviolet photodissociation mass spectrometry localizes cardiolipin unsaturations. *Anal. Chem.* **91**, 12509–12516
39. Macias, L. A., Garza, K. Y., Feider, C. L., Eberlin, L. S., and Brodbelt, J. S. (2021) Relative quantitation of unsaturated phosphatidylcholines using 193 nm ultraviolet photodissociation parallel reaction monitoring mass spectrometry. *J. Am. Chem. Soc.* **143**, 14622–14634
40. Klein, D. R., Feider, C. L., Garza, K. Y., Lin, J. Q., Eberlin, L. S., and Brodbelt, J. S. (2018) Desorption electrospray ionization coupled with ultraviolet photodissociation for characterization of phospholipid isomers in tissue sections. *Anal. Chem.* **90**, 10100–10104
41. Cody, R. B. B. S. F. (1979) Electron impact excitation of ions from organics: an alternative to collision induced dissociation. *Anal. Chem.* **51**, 547–551
42. Campbell, J. L., and Baba, T. (2015) Near-complete structural characterization of phosphatidylcholines using electron impact excitation of ions from organics. *Anal. Chem.* **87**, 5837–5845
43. Jones, J. W., Thompson, C. J., Carter, C. L., and Kane, M. A. (2015) Electron-induced dissociation (EID) for structure characterization of glycerophosphatidylcholine: determination of double-bond positions and localization of acyl chains. *J. Mass Spectrom.* **50**, 1327–1339
44. Baba, T., Campbell, J. L., Le Blanc, J. C. Y., and Baker, P. R. S. (2016) In-depth sphingomyelin characterization using electron impact excitation of ions from organics and mass spectrometry. *J. Lipid Res.* **57**, 858–867
45. Baba, T., Campbell, J. L., Le Blanc, J. C. Y., and Baker, P. R. S. (2016) Structural identification of triacylglycerol isomers using electron impact excitation of ions from organics (EIEIO). *J. Lipid Res.* **57**, 2015–2027
46. Baba, T., Campbell, J. L., Le Blanc, J. C. Y., and Baker, P. R. S. (2017) Distinguishing cis and trans isomers in intact complex lipids using electron impact excitation of ions from organics mass spectrometry. *Anal. Chem.* **89**, 7307–7315
47. Baba, T., Campbell, J. L., Le Blanc, J. C. Y., Baker, P. R. S., and Ikeda, K. (2018) Quantitative structural multiclass lipidomics using differential mobility: electron impact excitation of ions from organics (EIEIO) mass spectrometry. *J. Lipid Res.* **59**, 910–919
48. Pham, H. T., Ly, T., Trevitt, A. J., Mitchell, T. W., and Blanksby, S. J. (2012) Differentiation of complex lipid isomers by radical-directed dissociation mass spectrometry. *Anal. Chem.* **84**, 7525–7532
49. Narreddula, V. R., McKinnon, B. I., Marlton, S. J. P., Marshall, D. L., Boase, N. R. B., Poad, B. L. J., *et al.* (2021) Next-generation derivatization reagents optimized for enhanced product ion formation in photodissociation-mass spectrometry of fatty acids. *Analyst.* **146**, 156–169
50. Narreddula, V. R., Boase, N. R., Ailuri, R., Marshall, D. L., Poad, B. L. J., Kelso, M. J., *et al.* (2019) Introduction of a fixed-charge, photolabile derivative for enhanced structural elucidation of fatty acids. *Anal. Chem.* **91**, 9901–9909
51. Tomer, K. B., Crow, F. W., and Gross, M. L. (1983) Location of double-bond position in unsaturated fatty acids by negative ion MS/MS. *J. Am. Chem. Soc.* **105**, 5487–5488
52. Hsu, F. F., and Turk, J. (1999) Distinction among isomeric unsaturated fatty acids as lithiated adducts by electrospray ionization mass spectrometry using low energy collisionally activated dissociation on a triple stage quadrupole instrument. *J. Am. Soc. Mass Spectrom.* **10**, 600–612
53. Randolph, C. E., Foreman, D. J., Betancourt, S. K., Blanksby, S. J., and McLuckey, S. A. (2018) Gas-phase ion/ion reactions involving tris-phenanthroline alkaline earth metal complexes as charge inversion reagents for the identification of fatty acids. *Anal. Chem.* **90**, 12861–12869
54. Randolph, C. E., Blanksby, S. J., and McLuckey, S. A. (2020) Toward complete structure elucidation of glycerophospholipids in the gas phase through charge inversion ion/ion chemistry. *Anal. Chem.* **92**, 1219–1227
55. Li, P., Hoffmann, W. D., and Jackson, G. P. (2016) Multistage mass spectrometry of phospholipids using collision-induced dissociation (CID) and metastable atom-activated dissociation (MAD). *Int. J. Mass Spectrom.* **403**, 1–7
56. Takahashi, H., Shimabukuro, Y., Asakawa, D., Yamauchi, S., Sekiya, S., Iwamoto, S., *et al.* (2018) Structural analysis of phospholipid using hydrogen abstraction dissociation and oxygen attachment dissociation in tandem mass spectrometry. *Anal. Chem.* **90**, 7230–7238
57. Ma, X., and Xia, Y. (2014) Pinpointing double bonds in lipids by paternò-büchi reactions and mass spectrometry. *Angew. Chem. Int. Ed.* **53**, 2592–2596
58. Ma, X., Chong, L., Tian, R., Shi, R., Hu, T. Y., Ouyang, Z., *et al.* (2016) Identification and quantitation of lipid C=C location isomers: a shotgun lipidomics approach enabled by photochemical reaction. *Proc. Natl. Acad. Sci. U. S. A.* **113**, 2573–2578
59. Zhang, W., Zhang, D., Chen, Q., Wu, J., Ouyang, Z., and Xia, Y. (2019) Online photochemical derivatization enables comprehensive mass spectrometric analysis of unsaturated phospholipid isomers. *Nat. Commun.* **10**, 79
60. Zhang, W., Shang, B., Ouyang, Z., and Xia, Y. (2020) Enhanced Phospholipid isomer analysis by online photochemical derivatization and RPLC-MS. *Anal. Chem.* **92**, 6719–6726
61. Xia, T., Ren, H., Zhang, W., and Xia, Y. (2020) Lipidome-wide characterization of phosphatidylinositols and phosphatidylglycerols on C=C location level. *Anal. Chim. Acta.* **1128**, 107–115
62. Zhu, Y., Wang, W., and Yang, Z. (2020) Combining mass spectrometry with paternò–büchi reaction to determine double-bond positions in lipids at the single-cell level. *Anal. Chem.* **92**, 11380–11387
63. Ma, X., Zhang, W., Li, Z., Xia, Y., and Ouyang, Z. (2021) Enabling high structural specificity to lipidomics by coupling photochemical derivatization with tandem mass spectrometry. *Acc. Chem. Res.* **54**, 3873–3882
64. Esch, P., and Heiles, S. (2018) Charging and charge switching of unsaturated lipids and apolar compounds using Paternò-Büchi reactions. *J. Am. Soc. Mass Spectrom.* **29**, 1971–1980
65. Zhao, J., Fang, M., and Xia, Y. (2021) A liquid chromatography-mass spectrometry workflow for in-depth quantitation of fatty acid double bond location isomers. *J. Lipid. Res.* **62**, 100110
66. Cao, W., Cheng, S., Yang, J., Feng, J., Zhang, W., Li, Z., *et al.* (2020) Large-scale lipid analysis with C=C location and sn-position isomer resolving power. *Nat. Commun.* **11**, 375
67. Li, Z., Cheng, S., Lin, Q., Cao, W., Yang, J., Zhang, M., *et al.* (2021) Single-cell lipidomics with high structural specificity by mass spectrometry. *Nat. Commun.* **12**, 2869
68. Su, Y., Ma, X., Page, J., Shi, R., Xia, Y., and Ouyang, Z. (2019) Mapping lipid C=C location isomers in organ tissues by coupling photochemical derivatization and rapid extractive mass spectrometry. *Int. J. Mass Spectrom.* **445**, 116206
69. Tang, F., Guo, C., Ma, X., Zhang, J., Su, Y., Tian, R., *et al.* (2018) Rapid in situ profiling of lipid C=C location isomers in tissue using ambient mass spectrometry with photochemical reactions. *Anal. Chem.* **90**, 5612–5619
70. Bednarik, A., Bolsker, S., Soltwisch, J., and Dreisewerd, K. (2018) An on-tissue Paterno-Buchi reaction for localization of carbon-carbon double bonds in phospholipids and glycolipids by matrix-assisted laser-desorption-ionization mass-spectrometry imaging. *Angew. Chem. Int. Ed.* **57**, 12092–12096
71. Wäldchen, F., Mohr, F., Wagner, A. H., and Heiles, S. (2020) Multifunctional reactive MALDI matrix enabling high-lateral resolution dual polarity MS imaging and lipid C=C position-resolved MS2 imaging. *Anal. Chem.* **92**, 14130–14138
72. Zhao, Y., Zhao, H., Zhao, X., Jia, J., Ma, Q., Zhang, S., *et al.* (2017) Identification and quantitation of C=C location isomers of unsaturated fatty acids by epoxidation reaction and tandem mass spectrometry. *Anal. Chem.* **89**, 10270–10278
73. Cao, W., Ma, X., Li, Z., Zhou, X., and Ouyang, Z. (2018) Locating carbon–carbon double bonds in unsaturated phospholipids by epoxidation reaction and tandem mass spectrometry. *Anal. Chem.* **90**, 10286–10292
74. Tang, S., Cheng, H., and Yan, X. (2020) On-demand electrochemical epoxidation in nano-electrospray ionization mass spectrometry to locate carbon–carbon double bonds. *Angew. Chem. Int. Ed.* **59**, 209–214
75. Chintalapudi, K., and Badu-Tawiah, A. K. (2020) An integrated electrocatalytic nESI-MS platform for quantification of fatty acid isomers directly from untreated biofluids. *Chem. Sci.* **11**, 9891–9897
76. Feng, Y., Chen, B., Yu, Q., and Li, L. (2019) Identification of double bond position isomers in unsaturated lipids by m-CPBA

epoxidation and mass spectrometry fragmentation. *Anal. Chem.* **91**, 1791–1795
77. Kuo, T. H., Chung, H. H., Chang, H. Y., Lin, C. W., Wang, M. Y., Shen, T. L., *et al.* (2019) Deep lipidomics and molecular imaging of unsaturated lipid isomers: a universal strategy initiated by mCPBA epoxidation. *Anal. Chem.* **91**, 11905–11915
78. Song, C., Gao, D., Li, S., Liu, L., Chen, X., and Jiang, Y. (2019) Determination and quantification of fatty acid C=C isomers by epoxidation reaction and liquid chromatography-mass spectrometry. *Anal. Chim. Acta.* **1086**, 82–89
79. Bouza, M., Li, Y., Wu, C., Guo, H., Wang, Z. L., and Fernández, F. M. (2020) Large-area triboelectric nanogenerator mass spectrometry: expanded coverage, double-bond pinpointing, and supercharging. *J. Am. Soc. Mass. Spectrom.* **31**, 727–734
80. Swiner, D. J., Kulyk, D. S., Osae, H., Durisek Iii, G. R., and Badu-Tawiah, A. K. (2022) Reactive thread spray mass spectrometry for localization of c=c bonds in free fatty acids: applications for obesity diagnosis. *Anal. Chem.* **94**, 2358–2365
81. Zhou, Y., Park, H., Kim, P., Jiang, Y., and Costello, C. E. (2014) Surface oxidation under ambient air-not only a fast and economical method to identify double bond positions in unsaturated lipids but also a reminder of proper lipid processing. *Anal. Chem.* **86**, 5697–5705
82. Girotti, A. W. (1985) Mechanisms of lipid peroxidation. *Free Radic. Biol. Med.* **1**, 87–95
83. Unsihuay, D., Su, P., Hu, H., Qiu, J., Kuang, S., Li, Y., *et al.* (2021) Imaging and analysis of isomeric unsaturated lipids through online photochemical derivatization of carbon-carbon double bonds. *Angew. Chem. Int. Ed.* **60**, 7559–7563
84. Shindou, H., and Shimizu, T. (2009) Acyl-CoA: lysophospholipid acyltransferases. *J. Biol. Chem.* **284**, 1–5
85. Shindou, H., Hishikawa, D., Harayama, T., Yuki, K., and Shimizu, T. (2009) Recent progress on acyl CoA: lysophospholipid acyltransferase research. *J. Lipid Res.* **50**, S46–S51
86. Dennis, E. A., Cao, J., Hsu, Y. H., Magrioti, V., and Kokotos, G. (2011) Phospholipase A2 enzymes: physical structure, biological function, disease implication, chemical inhibition, and therapeutic intervention. *Chem. Rev.* **111**, 6130–6185
87. Inoue, A., and Aoki, J. (2006) Phospholipase A1: structure, distribution and function. *Future Lipidol.* **1**, 687–700
88. Ekroos, K., Ejsing, C. S., Bahr, U., Karas, M., Simons, K., and Shevchenko, A. (2003) Charting molecular composition of phosphatidylcholines by fatty acid scanning and ion trap MS3 fragmentation. *J. Lipid Res.* **44**, 2181–2192
89. Vogeser, M., and Schelling, G. (2007) Pitfalls in measuring the endocannabinoid 2-arachidonoyl glycerol in biological samples. *Clin. Chem. Lab. Med.* **45**, 1023–1025
90. Wang, M., Hayakawa, J., Yang, K., and Han, X. (2014) Characterization and quantification of diacylglycerol species in biological extracts after one-step derivatization: a shotgun lipidomics approach. *Anal. Chem.* **86**, 2146–2155
91. Yang, K., Dilthey, B. G., and Gross, R. W. (2016) Shotgun lipidomics approach to stabilize the regiospecificity of monoglycerides using a facile low-temperature derivatization enabling their definitive identification and quantitation. *Anal. Chem.* **88**, 9459–9468
92. Murphy, R., Leiker, T., and Robert, M. (2011) Glycerolipid and cholesterol ester analyses in biological samples by mass spectrometry. *Biochim. Biophys. Acta.* **1811**, 776–783
93. Herrera, L. C., Potvin, M. A., and Melanson, J. E. (2010) Quantitative analysis of positional isomers of triacylglycerols via electrospray ionization tandem mass spectrometry of sodiated adducts. *Rapid Commun. Mass Spectrom.* **24**, 2745–2752
94. Hsu, F. F., and Turk, J. (2010) Electrospray ionization multiple-stage linear ion-trap mass spectrometry for structural elucidation of triacylglycerols: assignment of fatty acyl groups on the glycerol backbone and location of double bonds. *J. Am. Soc. Mass Spectrom.* **21**, 657–669
95. Hsu, F. F., and Turk, J. (2003) Electrospray ionization/tandem quadrupole mass spectrometric studies on phosphatidylcholines: the fragmentation processes. *J. Am. Soc. Mass Spectrom.* **14**, 352–363
96. Pham, H. T., Maccarone, A. T., Thomas, M. C., Campbell, J. L., Mitchell, T. W., and Blanksby, S. J. (2014) Structural characterization of glycerophospholipids by combinations of ozone- and collision-induced dissociation mass spectrometry: the next step towards "top-down" lipidomics. *Analyst.* **139**, 204–214
97. Kirschbaum, C., Greis, K., Polewski, L., Gewinner, S., Schollkopf, W., Meijer, G., *et al.* (2021) Unveiling glycerolipid fragmentation by cryogenic infrared spectroscopy. *J. Am. Chem. Soc.* **143**, 14827–14834
98. Kozlowski, R. L., Mitchell, T. W., and Blanksby, S. J. (2015) A rapid ambient ionization-mass spectrometry approach to monitoring the relative abundance of isomeric glycerophospholipids. *Sci. Rep.* **5**, 9243
99. Marshall, D. L., Pham, H. T., Bhujel, M., Chin, J. S., Yew, J. Y., Mori, K., *et al.* (2016) Sequential collision-and ozone-induced dissociation enables assignment of relative acyl chain position in triacylglycerols. *Anal. Chem.* **88**, 2685–2692
100. Zhao, X., Zhang, W., Zhang, D., Liu, X., Cao, W., Chen, Q., *et al.* (2019) A lipidomic workflow capable of resolving sn- and C=C location isomers of phosphatidylcholines. *Chem. Sci.* **10**, 10740–10748
101. Zhao, X., and Xia, Y. (2021) Characterization of fatty acyl modifications in phosphatidylcholines and lysophosphatidylcholines via radical-directed dissociation. *J. Am. Soc. Mass Spectrom.* **32**, 560–568
102. Becher, S., Esch, P., and Heiles, S. (2018) Relative quantification of phosphatidylcholine sn-isomers using positive doubly charged lipid–metal ion complexes. *Anal. Chem.* **90**, 11486–11494
103. Taormina, V. M., Unger, A. L., Schiksnis, M. R., Torres-Gonzalez, M., and Kraft, J. (2020) Branched-chain fatty acids—An underexplored class of dairy-derived fatty acids. *Nutrients.* **12**, 2875
104. Ran-Ressler, R. R., Lawrence, P., and Brenna, J. T. (2012) Structural characterization of saturated branched chain fatty acid methyl esters by collisional dissociation of molecular ions generated by electron ionization. *J. Lipid Res.* **53**, 195–203
105. Wang, Z., Wang, D. H., Park, H. G., Tobias, H. J., Kothapalli, K. S. D., and Brenna, J. T. (2019) Structural identification of monounsaturated branched chain fatty acid methyl esters by combination of electron ionization and covalent adduct chemical ionization tandem mass spectrometry. *Anal. Chem.* **91**, 15147–15154
106. Wang, D. H., Wang, Z., and Brenna, J. T. (2020) Gas chromatography chemical ionization mass spectrometry and tandem mass spectrometry for identification and straightforward quantification of branched chain fatty acids in foods. *J. Agric. Food Chem.* **68**, 4973–4980
107. Wang, Z., Park, H. G., Wang, D. H., Kitano, R., Kothapalli, K. S., and Brenna, J. T. (2020) Fatty acid desaturase 2 (FADS2) but not FADS1 desaturates branched chain and odd chain saturated fatty acids. *Biochim. Biophys. Acta Mol. Cell Biol. Lipids.* **1865**, 158572
108. Poger, D., and Mark, A. E. (2015) A ring to rule them all: the effect of cyclopropane fatty acids on the fluidity of lipid bilayers. *J. Phys. Chem. B.* **119**, 5487–5495
109. Zetzsche, L. E., and Narayan, A. R. (2020) Broadening the scope of biocatalytic C–C bond formation. *Nat. Rev. Chem.* **4**, 334–346
110. Blevins, M. S., Klein, D. R., and Brodbelt, J. S. (2019) Localization of cyclopropane modifications in bacterial lipids via 213 nm ultraviolet photodissociation mass spectrometry. *Anal. Chem.* **91**, 6820–6828
111. Narreddula, V. R., Sadowski, P., Boase, N. R. B., Marshall, D. L., Poad, B. L. J., Trevitt, A. J., *et al.* (2020) Structural elucidation of hydroxy fatty acids by photodissociation mass spectrometry with photolabile derivatives. *Rapid Commun. Mass Spectrom.* **34**, e8741
112. Zhao, X., Wu, G., Zhang, W., Dong, M., and Xia, Y. (2020) Resolving modifications on sphingoid base and n-acyl chain of sphingomyelin lipids in complex lipid extracts. *Anal. Chem.* **92**, 14775–14782
113. Randolph, C. E., Foreman, D. J., Blanksby, S. J., and McLuckey, S. A. (2019) Generating fatty acid profiles in the gas phase: fatty acid identification and relative quantitation using ion/ion charge inversion chemistry. *Anal. Chem.* **91**, 9032–9040
114. Wäldchen, F., Spengler, B., and Heiles, S. (2019) Reactive matrix-assisted laser desorption/ionization mass spectrometry imaging using an intrinsically photoreactive Paterno–Buchi matrix for double-bond localization in isomeric phospholipids. *J. Am. Chem. Soc.* **141**, 11816–11820
115. West, H., and Reid, G. E. (2021) Hybrid 213 nm photodissociation of cationized Sterol lipid ions yield [M]+. radical products for improved structural characterization using multistage tandem mass spectrometry. *Anal. Chim. Acta.* **1141**, 100–109

116. Young, R. S. E., Bowman, A. P., Williams, E. D., Tousignant, K. D., Bidgood, C. L., Narreddula, V. R., *et al.* (2021) Apocryphal FADS2 activity promotes fatty acid diversification in cancer. *Cell Rep.* **34**, 108738
117. Xia, T., Yuan, M., Xu, Y., Zhou, F., Yu, K., and Xia, Y. (2021) Deep structural annotation of glycerolipids by the charge-tagging paterno–büchi reaction and supercritical fluid chromato graphy–ion mobility mass spectrometry. *Anal. Chem.* **93**, 8345–8353
118. Paine, M. R. L., Poad, B. L. J., Eijkel, G. B., Marshall, D. L., Blanksby, S. J., Heeren, R. M. A., *et al.* (2018) Mass spectrometry imaging with isomeric resolution enabled by ozone-induced dissociation. *Angew. Chem. Int. Ed.* **57**, 10530–10534
119. Feider, C. L., Macias, L. A., Brodbelt, J. S., and Eberlin, L. S. (2020) Double bond characterization of free fatty acids directly from biological tissues by ultraviolet photodissociation. *Anal. Chem.* **92**, 8386–8395
120. Wu, Q., Wang, J-Y., Han, D-Q., and Yao, Z-P. (2020) Recent advances in differentiation of isomers by ion mobility mass spectrometry. *TRAC Trends Anal. Chem.* **124**, 115801
121. Hinz, C., Liggi, S., and Griffin, J. L. (2018) The potential of Ion Mobility Mass Spectrometry for high-throughput and high-resolution lipidomics. *Curr. Opin. Chem. Biol.* **42**, 42–50
122. Kirschbaum, C., Saied, E. M., Greis, K., Mucha, E., Gewinner, S., Schöllkopf, W., *et al.* (2020) Resolving sphingolipid isomers using cryogenic infrared spectroscopy. *Angew. Chem. Int. Ed.* **59**, 13638–13642
123. Korf, A., Jeck, V., Schmid, R., Helmer, P. O., and Hayen, H. (2019) Lipid Species annotation at double bond position level with custom databases by extension of the MZmine 2 open-source software package. *Anal. Chem.* **91**, 5098–5105